Optimization and assessment of floating and floating-tracking PV systems integrated in on- and off-grid hybrid energy systems

Pietro Elia Campana[a,b,*], Louise Wästhage[a], Worrada Nookuea[a], Yuting Tan[b], Jinyue Yan[a,b]

[a] School of Business, Society and Engineering, Future Energy Center, Mälardalen University, 72123 Västerås, Sweden
[b] Department of Chemical Engineering, KTH – Royal Institute of Technology, 10044 Stockholm, Sweden

A B S T R A C T

Considering the targets of Thailand in terms of renewable energy exploitation and decarbonization of the shrimp farming sector, this work evaluates several scenarios for optimal integration of hybrid renewable energy systems into a representative shrimp farm. In particular, floating and floating-tracking PV systems are considered as alternatives for the exploitation of solar energy to meet the shrimp farm electricity demand.

By developing a dynamic techno-economic simulation and optimization model, the following renewable energy systems have been evaluated: PV and wind based hybrid energy systems, off-grid and on-grid PV based hybrid energy systems, ground mounted and floating PV based hybrid energy systems, and floating and floating-tracking PV based hybrid energy systems.

From a water-energy nexus viewpoint, floating PV systems have shown significant impacts on the reduction of evaporation losses, even if the energy savings for water pumping are moderate due to the low hydraulic head. Nevertheless, the study on the synergies between water for food and power production has highlighted that the integration of floating PV represents a key solution for reducing the environmental impacts of shrimp farming. For the selected location, the results have shown that PV systems represent the best renewable solution to be integrated into a hybrid energy system due to the abundance of solar energy resources as compared to the moderate wind resources. The integration of PV systems in off-grid configurations allows to reach high renewable reliabilities up to 40% by reducing the levelized cost of electricity. Higher renewable reliabilities can only be achieved by integrating energy storage solutions but leading to higher levelized cost of electricity. Although the floating-tracking PV systems show higher investment costs as compared to the reference floating PV systems, both solutions show similar competiveness for reliabilities up to 45% due to the higher electricity production of the floating-tracking PV systems. The higher electricity production from the floating-tracking PV systems leads to a better competitiveness for reliabilities higher than 90% due to lower capacity requirements for the storage systems.

1. Introduction

Two concerns growing along with the increase in energy demand are energy security and global warming. Renewable energy alternatives have been emphasized within many different business areas all around the world due to their capability of energy security enhancement and greenhouse gas mitigation in comparisons with conventional fossil fuels (Chimres and Wongwises, 2016). However, the major barrier of renewable alternatives is related to their high investment costs, while the fossil fuels cost remain lower. Therefore, not only the environmental perspective but also the economic profitability and the social wellbeing are needed to be considered for the evaluation of suitable alternatives (Kumar, 2016).

As with most of the Southeast Asian counties, Thailand is experiencing a rapid energy consumption increase due to population growth. The country has almost tripled the energy consumption within a period of 20 years (Huenteler et al., 2016). Currently, the country is the top two largest energy consumer in the Association of Southeast Asian Nations (ASEAN) (Department of Alternative Energy Development and Efficiency, 2014). Correspondingly, the greenhouse gas emission has almost doubled from the emission levels in 1990 since the majority of energy sources are fossil fuels (natural gas, oil, and coal). Moreover, the projections for the Thailand energy sector show that by 2035, the estimated imported fossil fuels will reach up to 90%. Therefore, energy security is a priority for the Government of Thailand. The overall goal of the national plans set by the Department of Alternative Energy

Development and Efficiency is to reach 25% renewable energy of the total energy consumption within the country by 2030 (Department of Alternative Energy Development and Efficiency, 2017). Hence, the installed renewable energy systems must increase rapidly in the near future to reach the national target, since the electrical demand will almost double by 2030 (Department of Alternative Energy, 2014).

Among the ASEAN countries, Thailand has one of the highest solar capacity potential, which makes the solar power one of the best renewable energy. The average solar irradiation in Thailand is 18.0 MJ/m^2/day (Chimres and Wongwises, 2016; Department of Alternative Energy Development and Efficiency, 2017). However, only 7.2% of the produced electricity are from the renewable energies in 2015 (Energy Policy and Planning Office, 2016). The feed-in-tariffs (FIT) policy has been implemented since 2007 by the Government of Thailand to encourage and support the private sector producers. The FIT programme covers the electricity produced from biomass, biogas, solar, wind, hydro and waste. The current average electricity price in Thailand is 0.1 US$/kWh. The FIT varies between 0.09 and 0.21 US$/kWh, depending on the technology. For ground mounted PV systems serving the agricultural or shrimp-farming sector, the FIT is approximately 0.16 US$/kWh (Electrical, 2013).

Thailand is one of the main aquaculture producer worldwide with 0.9 million tonnes in 2015 (Fishery and Aquaculture Statistics, 2017). In 2016, the country was the sixth biggest producer of shrimps and prawns worldwide with almost 330,000 t (Fisheries and Aquaculture Department). One of the major challenges of shrimp cultivation is the energy demand. Shrimp farming needs 24 h surface and bottom aeration. Intensive pumping is also needed to transfer large volumes of water from the sea to the water treatment ponds, the nursery ponds, the grow-out ponds, and for the slurry waste discharge. The intensive energy consumption does not only raise the operating cost but it is also associated with greenhouse gas emissions. Most of the farms are connected to the electrical grid. However, there is still a small percentage of shrimp farmers who still rely on diesel generators. The monthly electricity consumption of a shrimp farm was reported in the work carried out by Nookuea et al. (2016). A 6,400 m^2 single shrimp farm required in average 15–20 MWh/month mainly for aeration and water pumping. By installing solar PV systems to meet the required electricity consumption, the shrimp farms can become more energy self-sufficient, generate lower environmental impacts, and have better economic outcome due to the competitive levelized cost of electricity (*LCOE*). However, due to the low efficiency of solar PV modules, PV systems require large installation areas. This limitation can be overcome by the implementation of floating PV systems on the available water surface such as the surface of the water treatment pond.

As compared to the previous study carried out by Nookuea et al. (2016), this work aims to study the optimization of floating PV systems for shrimp farm cultivation in Thailand from an environmental, technical and economic viewpoint. At first, a short review of the cooling effects of floating PV systems is presented. The results of the review are then used in a techno-economic optimization model to study the effects of cooling on the optimization of hybrid energy systems for meeting the intensive energy requirements of a representative shrimp farm. This is done to also study how renewable energies can improve the sustainability of shrimp farming and thus support the shrimps market. The water-energy nexus aspects of floating PV systems are also investigated with special consideration to the reduction of evaporation losses and mutual use of water for power and food production, and wastewater treatment. This study also evaluates the advantages of integrating one-axis floating-tracking PV systems by providing the cost assessment for an unconfined floating structure. Different scenarios regarding the implementation of renewables into shrimp farming have been considered in this work, including ground mounted PV systems and wind turbine hybrid energy systems with storage, fixed floating and floating-tracking PV systems, and off- and on-grid solutions.

2. Floating PV systems literature review

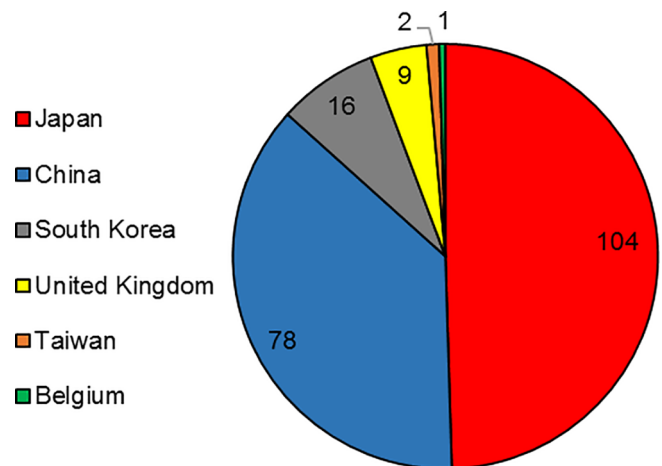In recent years, floating PV systems have gained more attention

Fig. 1. Installed capacity of the top 70 floating PV systems per country/region in 2018 (MWp) (Solarplaza, 2018).

from both a research point of view and a market perspective due to the direct and indirect benefits related to their installation (Sahu et al., 2016). At the end of 2016, the existing worldwide floating PV installed capacity was more than 94 MW$_p$. Japan represented 60% of the world installed capacity with 56 MW$_p$, followed by China (20 MW$_p$), United Kingdom (10 MW$_p$) and South Korea (6 MW$_p$) (NREL, 2018; Solar Asset Management, 2018). In 2018, the floating PV capacity reached 211 MW$_p$, only considering the top 70 floating PV installations worldwide as shown in Fig. 1 (Solarplaza, 2018). Japan has continued to lead the floating PV market thanks to the high FIT and lack of suitable land for large-scale PV systems.

Floating PV systems are marked out by a higher electrical efficiency due to the cooling effects of the water body on the solar panels. This increases the annual electricity production in combination also with an increased albedo and thus reflected solar radiation. Choi studied the performance of three floating PV systems on a reservoir in South Korea (Choi, 2014). The 2.4 kW$_p$ floating PV system reached an average conversion efficiency 7.6% higher than a reference ground mounted PV system. The 100 kW$_p$ floating PV system reached a conversion efficiency of 17.6%, 13.5% higher compared to the ground mounted PV system. The 500 kW$_p$ floating PV system reached an efficiency 10.3% higher than the reference PV system. Majid et al. carried out an experimental study by using a 80 W$_p$ floating PV system installed in a pond simulator, which showed an increase of the power gain from 5.9% up to 15.5% as compared to the reference ground mounted PV system (Majid et al., 2014). A summary of the cooling effects on the floating PV systems efficiency is presented in Table 1. In most of the works on the cooling effects of floating PV systems, very limited attention was given to those effects on the system optimization. In this study, we have focused on how the cooling effects can influence the system optimization.

Table 1
Summary of the cooling effect on the efficiency of floating PV systems.

Increased efficiency due to cooling effect compared to a reference ground mounted PV system	Refs.
7.6%, 13.5% and 10.3%	Choi (2014)
15.5%	Majid et al. (2014)
9%	Bahaidarah et al. (2013)
1.58–2.00%	Liu et al. (2017)
0.79%.	Yadav and Gupta, (2016)
2.82%–14.58%	Azmi et al. (2013)

From a water-energy nexus perspective, floating PV systems decrease evaporation rates from water bodies. In hot and dry climates, also considering the future adverse effects of climate changes on temperature and precipitation patterns, evaporation losses from water bodies represent a threat for the water resources management, in particular for irrigation purposes as well as for power production. Rosa-Clot et al. investigated the integration of floating PV systems in a wastewater treatment plant in Australia, focusing mainly on the avoided evaporation losses (Rosa-Clot et al., 2017). The authors concluded that floating PV systems can reduce evaporation losses ranging from 15,000 to 25,000 m^3/MW_p with further several electricity generation benefits as compared to ground mounted PV systems. Helfer et al. estimated that 40% of the reservoir water storage capacity is lost through evaporation in Australia (Helfer et al., 2012), and climate change projections on rising temperature could led to 15% higher evaporation losses. Bengoechea et al. estimated that evaporation losses in agricultural water reservoirs can reach up to 17% in Spain (Bengoechea et al., 1991). Santafé et al. calculated a water loss reduction of 25% after the installation of a floating PV system on a water irrigation reservoir in Spain (Santafé et al., 2014). Sahu et al. concluded that floating PV systems can prevent water storage capacity losses to up to 33% on natural lakes and ponds, and up to 50% on human-made water storage facilities (Sahu et al., 2016). A water-food-energy nexus approach was used by Pringle et al. in describing the concept of aquavoltaics that is the combination of floating PV systems with aquaculture (Pringle et al., 2017). The authors reviewed several applications in which the synergies between floating PV systems and aquaculture can be strengthened for water, energy and food security. From an environmental point of view, beside reducing CO_2 emissions as for other PV systems, floating PV systems can also decrease the algae growth and reduce the erosion of the bank by minimizing the negative effects of the waves. From an economic point of view, floating PV systems are also attractive because they do not require land for the installation, especially in areas where the cost of land represents an important item cost for the entire project investment. The environmental and economic aspects related to floating PV systems are particularly important for the shrimp farming sector because they represent a sustainable solution to the environmental pollution created by shrimp farms and the high cost of land (Nookuea et al., 2016; Engle et al., 2017). Most of the published studies have described the energy-water nexus concept and investigated only one part of the energy-water nexus. In this study, we have highlighted the relationships between the water losses and energy requirements for shrimp farms. Moreover, we have also highlighted the relationships among the combined use of water for food production, power production and wastewater treatment. These represent key issues for reducing the environmental impacts of shrimp farms both from a greenhouse gases point of view and from a water pollution point of view.

Similar to other solar tracking systems, floating-tracking PV systems can achieve higher electricity production as compared to fixed systems.

The tracking system follows the sun patterns to minimize the angle of incidence and thus maximize the direct fraction of the solar radiation hitting the PV surface. Contrary to ground based PV tracking systems, floating-tracking PV systems have greater rotation capacities (Choi et al., 2014a). One of the first floating-tracking PV system was installed in Italy in 2010, followed by the project at Lake Colignola in Italy in 2011 (Scienza Industria Tecnologia, 2017). Cazzaniga et al. recently presented a review on the performances and design solutions of floating PV systems (Cazzaniga et al., 2018). The authors provided a comparison between submerged and floating PV systems, and analysed different supporting structure designs, including floating-tracking PV system, and cooling techniques. The authors reported the performances analysis of two floating PV systems operating in Italy. The authors also presented an interesting floating-tracking solution without confinement. This cost effective solution consisted of connecting the centre of the floating platform to a submersible concrete anchor through a mooring chain. The rotation was guaranteed through a sun-tracking algorithm that drives submerged propellers. The solution was implemented and tested for a pilot floating PV systems in Italy. A schematic diagram of a floating-tracking solution without confinement is presented in Fig. 2.

Several other studies have focused on the detailed structural design of floating PV systems (Kim et al., 2017; Lee et al., 2014) and floating-tracking PV system structures (Choi et al., 2014b; Choi et al., 2014c). Nevertheless, few studies have focused on the economic aspects related to the implementation of floating-tracking structures. From an energy system point of view, in a recent study conducted by Silvério et al. (2018), the authors studied the coordinated operation of hydroelectric and floating PV power plants in the São Francisco River basin. The authors concluded that the integration of floating PV systems could increase the capacity factor of hydroelectric power plants by 17.3% with the potential effects of replacing thermal power plants. Trapani and Millar studied the integration of off-shore floating thin-film PV systems in Malta (Trapani and Millar, 2013) with special consideration to optimal capacity designs and CO_2 emission reductions. An interesting energy system aspect addressed by the authors was the study on the maximum capacity of floating PV systems allowed by the island power system if no interconnection with Sicily was finalized. Cazzaniga et al. have also studied the integration of compressed air energy storage into floating PV systems and wastewater treatment plants to explore the synergies and develop novel system concepts (Cazzaniga et al., 2017; Rosa-Clot et al., 2017). In recent years, there have been several studies on hybrid energy systems for both off-grid and on-grid applications, of which most of the works focused on the optimal design of the system components (Luna-Rubio et al., 2012). Shi et al. used a preference-inspired coevolutionary algorithm to solve a multi-objective optimization problem for a hybrid PV-wind-diesel-battery system to minimize the annual cost of the system, the loss of power supply probability, and emissions (Shi et al., 2015). The model predictive control showed better performances as compared to open-loop control system. Kaabeche et al.
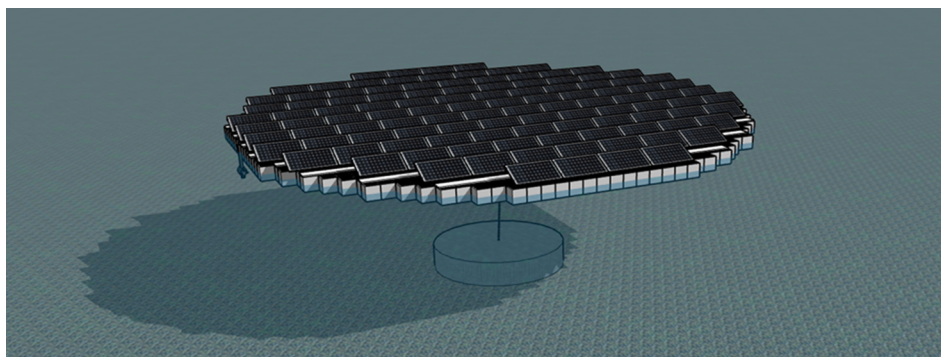

Fig. 2. Schematic diagram of a floating-tracking PV system solution.

adopted the Firefly Algorithm for the optimization of a hybrid PV-wind-diesel-battery system (Kaabeche et al., 2017). The authors found that the proposed algorithm had better performances as compared to other well-known algorithms such as Accelerated Particle Swarm Optimization, Generalized Evolutionary Walk and Bat in solving the optimization problem. Tazvinga et al. focused on developing an energy dispatch model using model predictive control techniques in a hybrid PV-wind-diesel-battery system (Tazvinga et al., 2014). The authors showed the robustness of the model in dealing with disturbances. Few studies have investigated the optimal capacity selection of the system components during the optimization process. Using a multi-objective optimization algorithm, in this work we have analysed the mutual relationships between objectives and the selected capacities (decisional variables) of the system components. In particular, we have analysed how different energy management strategies, both for on- and off-grid hybrid energy systems, and the effects of cooling can affect the selection of decisional variables, in particular PV and battery capacities.

3. System description

There are three main phases for the cultivation of shrimps, which are hatchery, nursery and grow-out phase. Typically, the hatchery phase is performed by the hatchery farms. The shrimp larvae are then sold to the grow-out farms for nursery and grow-out phase. For all phases, the most energy intensive operations are the aeration and water pumping. Shrimp farms need a secure and sufficient power supply, which is not subject to lengthy power failures. Moreover, an on-site emergency generator is of critical importance to ensure that the key operations can continue functioning during power blackouts. Among these three phases, the grow-out phase is the most energy intensive. For the Pacific white shrimp, the nursery and grow-out periods last around 90 days. The shrimp larvae are first reared in the indoor nursery tank with a bottom aeration system. This phase requires around 20–30 days before the juvenile shrimps are transferred to the full-size grow-out pond. In the grow-out pond, both surface and bottom aeration are required 24 h a day to maintain dissolved oxygen levels sufficiently high. The wastewater from the shrimp grow-out pond can be fed to the nearby fishpond for the preliminary treatment. Detailed descriptions of

the shrimp farm used in this work and the corresponding renewable configurations that can be undertaken to increase the energy sustainability of the process are presented in Fig. 3. The shrimp farm is located in Nakhon Si Thammarat (8.4 N, 100.0 E). To avoid negative effects on the shrimp farm cultivation, only the water treatment pond has been considered as a potential site for the floating PV installation. The pond area is 3,600 m².

The required electrical load was calculated based on a system with two grow-out ponds operating partly in parallel (one nursery pond, and one water treatment pond). Most of the load is from the motors used to drive the propellers for surface aeration and the pumping system for filling the water in the ponds. The overall system consumes more electricity during the night-time due to the decline of oxygen, and also because the pond is filled at night. The load for the bottom aeration for both the grow-out and the nursery ponds represents a minimal part of the load. By including the wastewater treatment load, the energy consumption profile of the entire system changes significantly. The load for the wastewater treatment was calculated based on the weight of produced shrimp as reported in Sun, 2009. The monthly electricity consumption profile is depicted in Fig. 4.
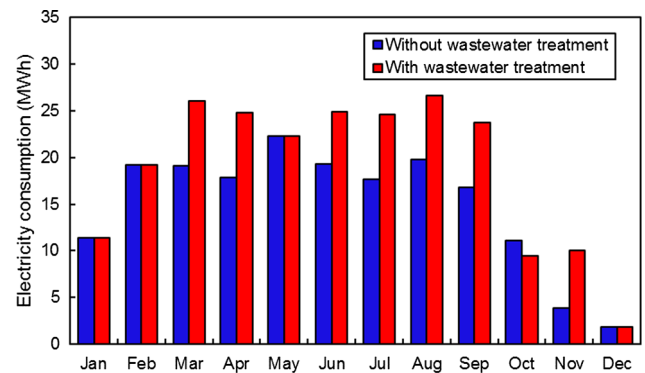

Fig. 4. Monthly electricity consumption profile of the representitive shrimp farm with and without wastewater treatment.
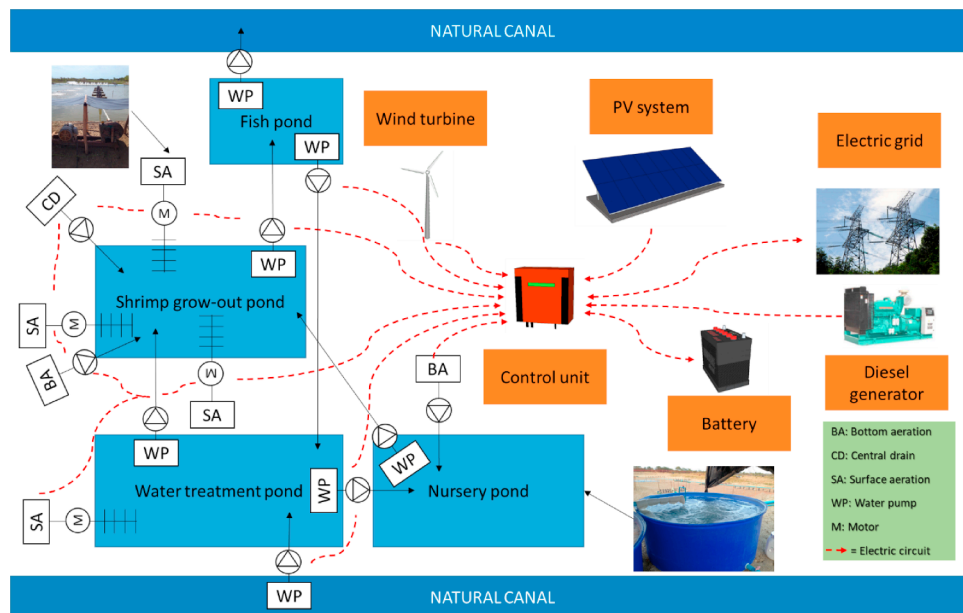

Fig. 3. Shrimp farm layout, main loads and suggested renewable energies integration.

4. Methodology

4.1. Evaporation

The hourly evaporation from shallow water bodies has been calculated from the reference evapotranspiration ET_0 using the Penman-Monteith equation (Allen et al., 1998):

$$ET = K_w \frac{0.408\Delta(R_n - G) + \gamma\frac{37}{T_a + 273}u_2(e_s - e_a)}{\Delta + \gamma(1 + 0.34u_2)} \tag{1}$$

where K_w is the open water coefficient, R_n is the hourly net radiation at the water surface (MJ/m^2), G is the hourly soil heat flux density (MJ/m^2), T_a is the mean hourly air temperature (°C), Δ is the saturation slope of vapor pressure curve at T_a (kPa/°C), γ is the psychrometric constant (kPa/°C), e_s is saturation vapour pressure (kPa), e_a is the average hourly actual vapour pressure (kPa), and u_2 is the average hourly wind speed (m/s). K_w has been assumed equal to 1.05 as suggested by Allen et al. (1998). The hourly evaporation pattern for the selected site has been calculated using Eq. (1) with the hourly climatic parameters taken from the global meteorological database Meteonorm, 2017. The evaporation negatively affects the daily energy requirements for water pumping in two different ways: reducing the downstream water head, thus increasing the total pumping head, and increasing the water volume losses. The resulting daily electricity demand $\Delta E_{el,i}$ (kWh) to maintain stable the water level in the ponds of the shrimp farm is given by the following equation:

$$\Delta E_{el,i} = \frac{0.0027\Delta V_{w,i}\Delta TDH_i}{\eta_{ps}} \tag{2}$$

where 0.0027 is a conversion factor between Joule and kWh considering the density of water (1,000 kg/m^3) and the gravity acceleration (9.8 m/s^2), $\Delta V_{w,i}$ is the daily water volume lost due to evaporation, ΔTDH_i is the daily variation of the total dynamic head (m), mainly due to the variation of the geodetic head ΔH_g (m), and η_{ps} is the efficiency of the pumping system (%). A schematic diagram of the hydraulic heads and related variations due to evaporation losses is depicted in Fig. 5 considering the natural canal, the water treatment pond and the shrimp grow-out pond.

4.2. Simulation models

This section shortly describes the energy system models used in this work, in particular the solar PV system, the wind turbine, the battery, and the diesel generator used as back-up in off-grid systems.

4.2.1. PV model

The PV model calculates the solar energy converted into electricity through PV modules. The global solar radiation has been calculated considering the beam, diffuse and reflected radiation using the methods described in Duffie and Beckman, 2013. For the fixed PV systems, the angle of incidence has been calculated by using following equation (Duffie and Beckman, 2013):

$$cos\theta = sin\theta_z sin\beta cos(\gamma_s - \gamma) + cos\theta_z cos\beta \tag{3}$$

where θ_z is the zenith angle (°), β is the tilt angle of the module (°), γ_s is the solar azimuth angle (°), and γ is the surface azimuth angle (°). For PV systems tracking the sun while rotating around a vertical axis with a fixed tilt angle, the angle of incidence θ is given by the following equation (Duffie and Beckman, 2013):

$$cos\theta = cos\theta_z cos\beta + sin\theta_z sin\beta \tag{4}$$

The efficiency of the PV system η_{PV} (%) has been calculated using the following equation (Duffie and Beckman, 2013):

$$\eta_{PV} = \eta_{PV,STC}\left(1 + \frac{\mu}{\eta_{PV}}(T_a - T_{STC}) + \frac{\mu}{\eta_{PV,STC}}\frac{a + bv_{NOCT}}{a + bv}\frac{NOCT - 20}{800}(1 - \eta_{PV,STC})G_t\right)\Psi \tag{5}$$

where $\eta_{PV,STC}$ is the standard test condition (STC) efficiency of the PV module (%), μ is the temperature coefficient of the power output (%/°C), T_a is the ambient temperature (°C), T_{STC} is the STC temperature (25°C), v_{NOCT} is the wind speed at the nominal operating cell temperature (NOCT) (m/s), v is the actual wind speed (m/s), a and b are coefficients, G_t is the global incident radiation on the PV array (W/m^2), and Ψ is a correction factor to take into account the cooling effect. The potential cooling effect of solar floating PV systems on the PV efficiency refers to the previous theoretical and experimental studies summarized in Table 1. The reference PV module is Yingli YL250P-29b (Yingli Solar, 2018).
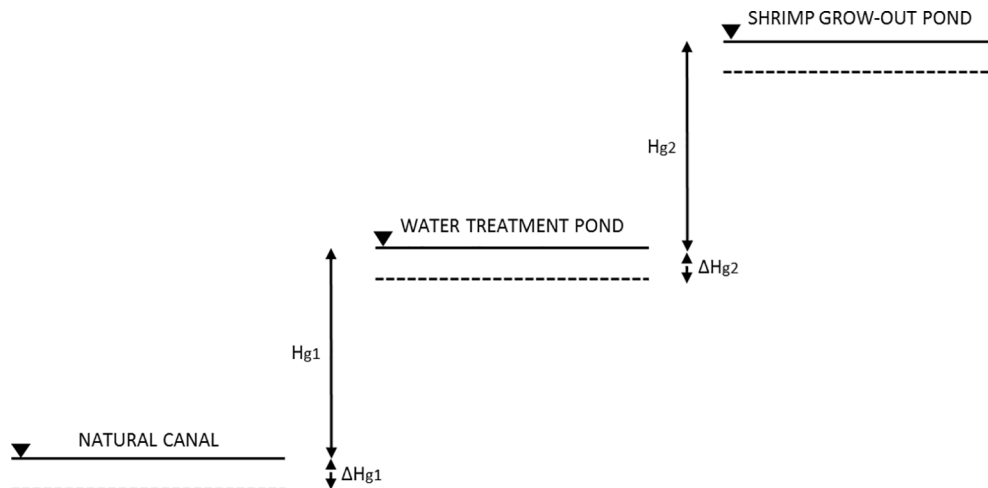

Fig. 5. Hydraulic scheme of the natural canal, water treatment pond and shrimp grow-out pond with the related change of the geodetic heads due to evaporation.

4.2.2. Wind turbine

The wind turbine power output P_{WT} (kW) has been modeled with the following set of equations that describes the characteristic wind turbine power curve (Lydia et al., 2014):

$$P_{WT} = \begin{cases} 0(\nu < \nu_i \, and \, \nu > \nu_0) \\ \frac{1}{2}\rho A C_p \nu^3 (\nu_i \le \nu \le \nu_r) \\ P_{WT,r}(\nu_r \le \nu \le \nu_0) \end{cases} \tag{6}$$

where ν is the actual wind speed (m/s), ν_i, ν_r and ν_0 are the cut-in, rated and cut-out characteristic speeds of the wind power curve (m/s), ρ is the air density (kg/m^3), A is the rotor area (m^2), C_p is the power coefficient, and $P_{WT,r}$ is the wind turbine rated power (kW). The values assumed for ν_i, ν_r, ν_0, A, and C_p are 3.5 m/s, 13.5 m/s, 25.0 m/s, 572 m^2, and 0.46 respectively. Those values refer to the wind turbine ACSA A27/225 as reported in Carrillo et al. (2013).

4.2.3. Diesel generator

In case of off-grid power systems, the back-up power is provided by a diesel generator. The fuel consumption of the diesel generator has been calculated with the following equation (Ismail et al., 2013):

$$FC_{diesel} = \alpha * P_{DG} + \beta * P_{DG,r} \tag{7}$$

where α and β are the experimental coefficients of the fuel consumption curve, 0.246 and 0.08145 respectively (Ismail et al., 2013). P_{DG} is the power output from the diesel generator to cover the load (kW), and $P_{DG,r}$ is the rated power output of the diesel generator, assumed 25% higher than the maximum annual power requirement (kW) on hourly basis.

4.2.4. Battery

The battery energy capacity (BEC) (kWh) has been calculated by using an energy balance model described by the following equation:

$$\frac{d(BEC)}{dt} = (P_p - P_c) * \eta - E_{loss} \tag{8}$$

where dt is the simulation time step (1 h), E_{loss} represents the energy lost due to the self-discharge rate (kWh), η is the efficiency of the charging-discharging process (%), P_{ip} and P_c are the power production and consumption during the time step (kW). The hourly self-discharge rate and the battery charging-discharging efficiency have been assumed equal to 0.02% and 85% respectively (Kanase-Patil et al., 2011). The BEC varies between an upper and lower value, BEC$_{MAX}$ and BEC$_{MIN}$. If the battery reach its maximum energy capacity, the power surplus is exported to the grid or dumped. Otherwise, if the battery is at its lowest energy capacity, the load is covered by the electrical grid for on-grid systems or by the diesel generator for off-grid systems.

4.3. Optimization

The optimization has been carried out with the open-source code OptiCE written in Matlab® environment (OptiCE, 2018). The model uses genetic algorithm (GA) as optimization method to solve single or multi-objective optimization problems. In this study, the code is set to minimize the LCOE, while maximizing the energy system reliability (REL) (%). The LCOE has been defined from the life cycle cost (LCC) (US $) calculation and life cycle electricity production as follows:

$$LCOE = \frac{LCC}{\sum_{n=1}^{N} E_{el} \frac{(1-r)^n}{(1+d)^n}} \tag{9}$$

where E_{el} is the initial annual electricity production (kWh), r is the degradation rate (%) and d is the real discount rate (%). $E_{el,n}$ for off-grid systems is calculated as sum of the net electricity produced by the renewable energies (defined as difference between electricity produced and electricity dumped) and diesel generator. This is to avoid overdesign of the renewables capacities and thus overproduction. The real

discount rate d used in the calculation of the LCC has been calculated with the following equation:

$$d = \frac{d' - f}{1 + f} \tag{10}$$

where d' is the discount rate (%) and f is the inflation rate (%). The reliability REL (%) has been defined as follows:

$$REL = \frac{H_{REN+BATT}}{8760} * 100 \tag{11}$$

where $H_{REN+BATT}$ is the number of hours the renewable energies supported by the energy storage system can cover the load during the year (h). The calculation of the land required for the installation of the PV system, and thus the potential installed peak power, has been performed considering the land packing factor (PF), defined as the ratio between PV area and land area required for the installation of the PV system and given by the following equation (Martín-Chivelet, 2016):

$$PF = \left(\cos\beta + \frac{\sin\beta}{\tan(90 - \theta_z)}\cos\gamma_s\right)^{-1} \tag{12}$$

The tilt angle β has been assumed equal to 8° (corresponding to the latitude of the shrimp farm). Eq. (12) has been applied at noon of the winter solstice (Martín-Chivelet, 2016). The area calculated by using Eq. (12) has been increased of 2 m^2/kW$_p$ for the secondary floating platform for maintenance. This corresponds to a required installation area of 10 m^2/kW$_p$. Santafé et al. reported similar values for Spain (Santafé et al., 2014). The optimization problem is based on six decisional variables: tilt angle (°), azimuth angle (°), PV capacity (kW$_p$), wind tower height (m), wind power capacity (kW$_r$), and battery energy capacity (kWh). The lower and upper bounds of the decisional variables are summarized in Table 2. The upper bound for the PV power capacity has been set to 200 kW$_p$ based on the water surface available for the floating PV system in the water treatment pond. Accordingly, the upper bound of the wind power capacity has been set equal to 200 kW$_r$.

The main input economic data for the optimization are summarized in Table 3, while the specific breakdown costs for the different PV systems configurations are given in Table 4.

As regards the PV module costs, the 2015 National Survey Report of PV Power Applications in Thailand reported an average price of about 0.7 US \$/W$_p$, with the lowest and highest equal to 0.6 and 0.8 US\$/W$_p$ (DEDE, 2015). In this study, we used 0.7 US\$/W$_p$ as a reference specific cost. To avoid site-specific results, sensitivity analyses have been carried out considering the variation of the cost for the land and the floating structure, especially in Section 5.2.3 when comparing ground mounted and floating PV systems. In the period 2012–2015, the specific cost of the land in Nakhon Si Thammarat province varied between 15 US\$/m^2 up to 625 US\$/m^2 (Nation Blog, 2017). In the period 2016–2018, according to the Treasury Department's, the average price of the land in Nakhon Si Thammarat province has varied between 2.3 and 77.5 US\$/m^2 (Treasury Department, 2018). The high variation of the cost of land for shrimp farming is due to several factors, such as the distance from the sea, main road, water canal and electrical grid, and the possibility to use the land also for other purposes. The high cost of land is also connected to the high income of shrimp farming and related speculation (Engle et al., 2017). A reference cost of 50 US\$/m^2 was used in this study. The sensitivity analyses have been

Table 2
Decisional variables upper and lower bounds.

Decisional variables	Lower bound	Upper bound
Tilt angle (°)	0	30
Azimuth angle (°)	−10	10
PV capacity (kW$_p$)	0	200
Wind tower height (m)	0	80
Wind power capacity (kW$_r$)	0	200
Battery capacity (kWh)	0	4000

Table 3
Economic input data for the optimization.

Economic parameter	Value	Refs./Comment
Specific cost of ground mounted PV system (US$/kW)	2000	See Table 4
Specific cost of floating PV system (US$/kW)	2350	See Table 4
Specific cost of floating-tracking PV system (US$/kW)	2410	See Table 4
Specific cost of wind turbine (US$/kW)	1700	IRENA (2014)
Specific cost of battery (US$/kWh)	500	Lazard (2017)
Specific cost of diesel generator (US$/kW)	1000	Merei et al. (2013)
Specific cost of diesel (US$/l)	0.85	Global Petrol Prices (2018)
Specific cost of electricity bought from national grid (US$/kWh)	0.1	Thailand (2016)
Specific cost of electricity surplus sold to national grid with FIT (US$/kWh)	0.17	Thailand (2016)
Project lifetime (years)	25	Based on the system's component with longest lifetime
PV system lifetime (years)	25	Khiareddine and Salah, (2018)
Wind turbine lifetime (years)	25	Khiareddine and Salah, (2018)
Battery lifetime (years)	10	Lazard (2017)
Inverter lifetime (years)	10	Kaabeche and Ibtiouen (2014)
Diesel generator lifetime (years)	5	Refer to a prime-power, liquid-cooled diesel. Adapted from HOMER (2018)
Tax rate (%)	20	Trading Economics (2017)
Discount rate (%)	2.1	Trading Economics (2017) 10 years average
Inflation rate (%)	1.9	Trading Economics (2017) 10 years average
Maintenance rate of PV system (%)	2	Merei et al. (2013)
Maintenance rate of wind turbine (%)	2	Merei et al. (2013)
Maintenance rate of battery (%)	2	Lazard (2017)
Maintenance rate of diesel generator (%)	2	Merei et al. (2013)

Table 4
Specific breakdown costs for the reference PV systems configurations.

Component	Ground mounted PV	Floating PV	Floating-tracking PV
PV module (US$/kW$_p$)	700 DEDE (2015)	700 DEDE (2015)	700 DEDE (2015)
Inverter (US$/kW$_p$)	150 DEDE (2015)	150 DEDE (2015)	150 DEDE (2015)
Other hardware costs (including racking and wiring) (US$/kW$_p$)	150 DEDE (2015)	150 DEDE (2015)	150 DEDE (2015)
Land (US$/m^2)	50 (DEDE, 2015; Nation Blog, 2017)	–	–
Floating structure, mooring and anchoring (US$/m^2)	–	85 Santafé et al. (2014)	85 Santafé et al. (2014)
Tracking system (US$/kW$_p$)	–	–	12,000 (see Appendix A)
Installation labour (US$/kW$_p$)	300 DEDE (2015)	300 DEDE (2015)	300 DEDE (2015)
Profit (US$/kW$_p$)	150 DEDE (2015)	150 DEDE (2015)	150 DEDE (2015)
Others soft costs (including contracting, permitting and financing) (US$/kW$_p$)	50 DEDE (2015)	50 DEDE (2015)	50 DEDE (2015)
Investment cost (US$/kW$_p$)	1500 (without land) 2000 (with land at 50 US$/m^2)	2350	2410

performed by varying the land cost from 20 to 200 US$/m^2. A further scenario concerning the effect of the land rental instead of land ownership on the economy of PV systems has been considered. The annual land rental has been estimated as 5% of the land value. The cost variation for the floating structure has been assumed equal to ± 50% of the cost reported by Santafé et al. (2014). As concerns the floating-tracking PV system structure, the solution described in Cazzaniga et al. (2018) and depicted in Fig. 2 has been selected in this study. This solution is cost-effective and easy to implement in an extremely confined water body, as the wastewater treatment pond of the shrimp farm. The calculations of the floating-tracking platform are described more in details in the Appendix.

4.4. Scenarios definition

A summary of the scenarios (S1-4) with the related hybrid energy

Table 5
Summary of the investigated scenarios.

Description	Scenarios			
	S1	S2	S3	S4
Ground mounted PV	–	x	–	–
Floating PV	–	–	x	–
Floating-tracking PV	–	–	–	x
Wind turbine	x	–	–	–
Battery	x	x	x	x

system components taken into consideration in the simulations and optimizations is given in Table 5. Scenario S1 concerns the integration of an off-grid wind-diesel-battery system (WT + BATT + DG) in the representative shrimp farm. Scenario S2 considers the integration of an off-grid PV-diesel-battery system (PV + BATT + DG) to cover the electricity requirements of the shrimp farm. A sub-scenario for S2 has been also considered and it refers to a grid-connected hybrid energy system. For this sub-scenario, the optimization objective of maximizing the reliability REL (%) is changed with the objective of maximizing the renewable penetration (RP) (%) by assuming that the electrical grid has a reliability of 100%. In scenario S3, the ground mounted PV system of scenario S2 is replaced with a fixed floating PV system. The last scenario analyses the integration of one-axis floating-tracking PV systems into the off-grid hybrid energy system. While analysing those scenarios, several sensitivity analyses have been conducted. These sensitivity analyses have mainly concerned the impact of the cooling effect and components' investment costs on the system optimization.

5. Results and discussion

5.1. Evaporation losses and water-energy nexus aspects connected to floating PV systems

The hourly trend of evaporation losses from the water body at the selected location during the whole year is depicted in Fig. 6. The total annual evaporation losses account for about 1,100 mm (i.e. 11,000 m^3 of water losses each hectare of water body). Given the geometrical
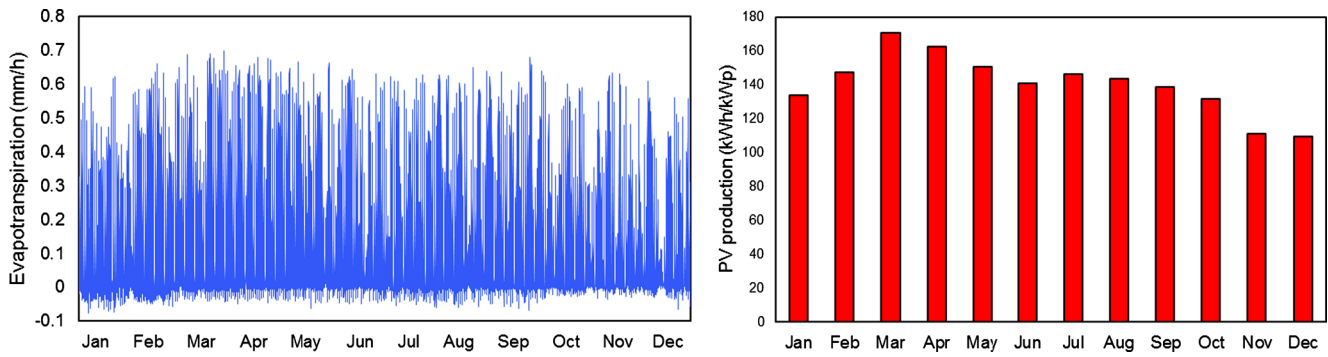
Fig. 6. Hourly evaporation from the water treatment pond (left) and monthly specific PV electricity production (right).

dimension of the investigated water treatment pond for shrimp cultivation and assuming an overall pumping efficiency of 60%, the annual water losses account for about $3,800 \, m^3$ that corresponds to about 100 kWh of electricity required to maintain the water level constant during the year. According to Sahu et al., floating PV systems can prevent water storage capacity losses up to 50% on human-made water storage facilities (Sahu et al., 2016). Thus, the floating PV system and the floating-tracking PV system (assumed maximum $200 \, kW_p$ to allow the normal operation of the shrimp farm) can potentially avoid about $1,050 \, m^3$ of water losses corresponding to about 25 kWh of electricity for water pumping. Although the avoided water losses are significant, the electricity savings for water pumping and the related CO_2 emissions are minimal mainly due to the low pumping head. Although in the selected shrimp farm the head difference between the natural canal and the water treatment pond has been assumed constant, in real conditions the geodetic head increases due to the evaporation losses. This can affect the energy consumption for water pumping in two different ways: due to the increase of the total dynamic head (linear effect), and the different pump efficiency at different hydraulic head operating conditions (non-linear effect). Although the water-energy nexus results for the shrimp farm show that the energy savings due to the reduced evaporation are minimal, from a regional or sector perspective they can be significant. Indeed, shrimp aquaculture involves more than 20,000 shrimp farms across the country (Portley, 2016). The use of water for the combined production of food and electricity is a key aspect for the water-food-energy nexus that allows reducing the environmental impact of shrimp farming. As seen in Fig. 4, the annual electricity consumption of the shrimp farm is around 230 MWh of which 45 MWh are due to the wastewater treatment. The annual electricity production of the assumed $200 \, kW_p$ PV system can actually offset the annual electricity demand of the shrimp farm. This allows producing a near carbon-free product with high economic value in the market chain due to environmental labelling. It is worth noting that the surplus of electricity production can generate further revenues in on-grid systems due to the possibility of electricity trading with the national grid. In both on- and off-grid systems, the surplus of power can be dumped through the aeration and related wastewater treatment processes to further improve the quality of the effluent.

5.2. Optimization

5.2.1. Hybrid energy system: Wind turbine and ground mounted PV system (S1 and S2)

The relationship between the *LCOE* and the *REL* for two off-grid hybrid energy systems (PV system, battery and diesel generator (PV + BATT + DG) and wind turbine, battery and diesel generator (WT + BATT + DG)) is depicted in Fig. 7. The relationship between *LCOE* and *REL* represents the Pareto front of the optimization problem. By increasing the *REL* for the PV + BATT + DG off-grid system, the *LCOE* initially decreases until 40% *REL*. Afterwards, the *LCOE* starts to
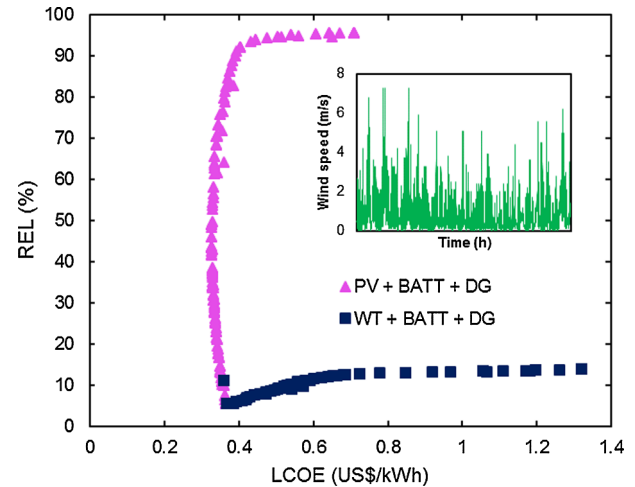

Fig. 7. Pareto front for the off-grid hybrid PV and WT energy systems.

increase until 90%. To reach higher *REL* than 90%, the *LCOE* dramatically increases. The optimization of the hybrid WT + BATT + DG system shows a rapid increase of the *LCOE* at very low *REL* that never exceeds the 15%. This is due to the low wind speeds at selected location, as superimposed in Fig. 7 (wind speeds at 10 m height), and thus low wind turbine power output. The Pareto fronts shown in Fig. 7 can be explained more in details by analysing the trend of the PV and battery capacities selection against the *REL* during the optimization process for the PV + BATT + DG off-grid system, as shown in Fig. 8 (right). Similarly, the trend of wind turbine and battery capacities for the WT + BATT + DG off-grid system is shown in Fig. 8 (left).

As it can be seen, for the PV + BATT + DG off-grid system the *REL* initially increases due to the increase in capacity of the PV system until 40% *REL*. Afterwards, higher *REL* are achieved by increasing the battery capacity. As concerns the WT + BATT + DG off-grid system, a *REL* of about 8% is achieved by selecting immediately the wind turbine capacity to values close to the upper boundary of $200 \, kW_r$. Further minor increase of the *REL* are achieved by increasing the battery capacity up to the maximum values set in the optimization problem. Due to the low/moderate winds (average annual wind speed at 10 m height lower than 1 m/s), by increasing the wind turbine capacity or increasing the battery capacity to store the energy surplus has an insignificant effect on the *REL*. Thus, most of the energy requirements are fulfilled by the diesel generator.

From the spatial maps of the annual average solar irradiation and wind speed, shown in Fig. 9, it can be clearly deducted that the results concerning the comparison between PV + BATT + DG and WT + BATT + DG off-grid systems have a national validity. Indeed, the average wind speed map shows very low/moderate wind conditions in almost all the country. Similar low/moderate wind speed conditions
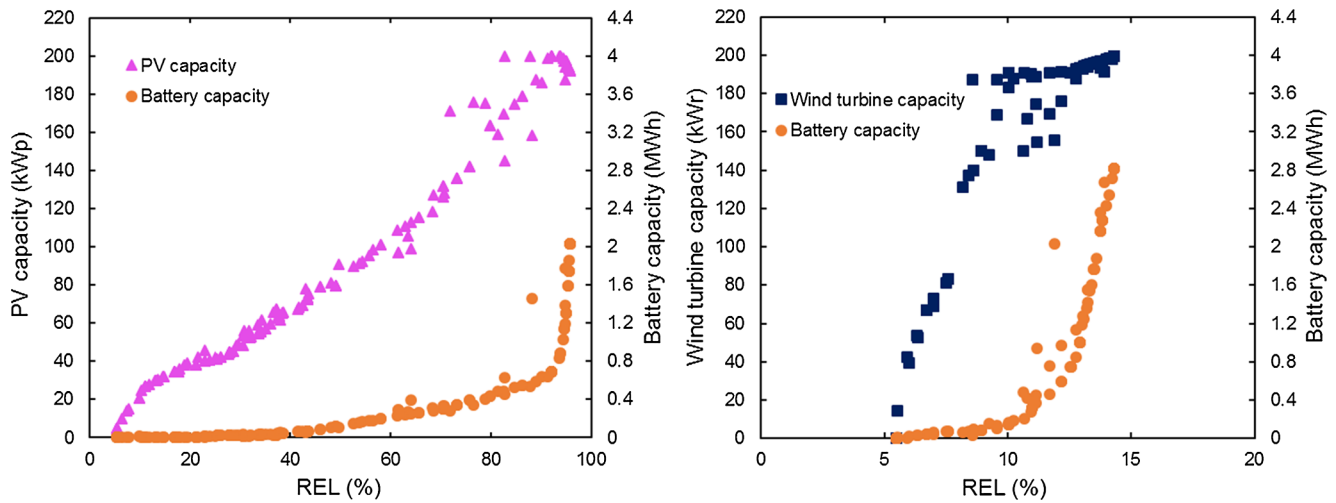
Fig. 8. Relationship between PV (left), wind turbine (right) and battery capacities with the reliability.
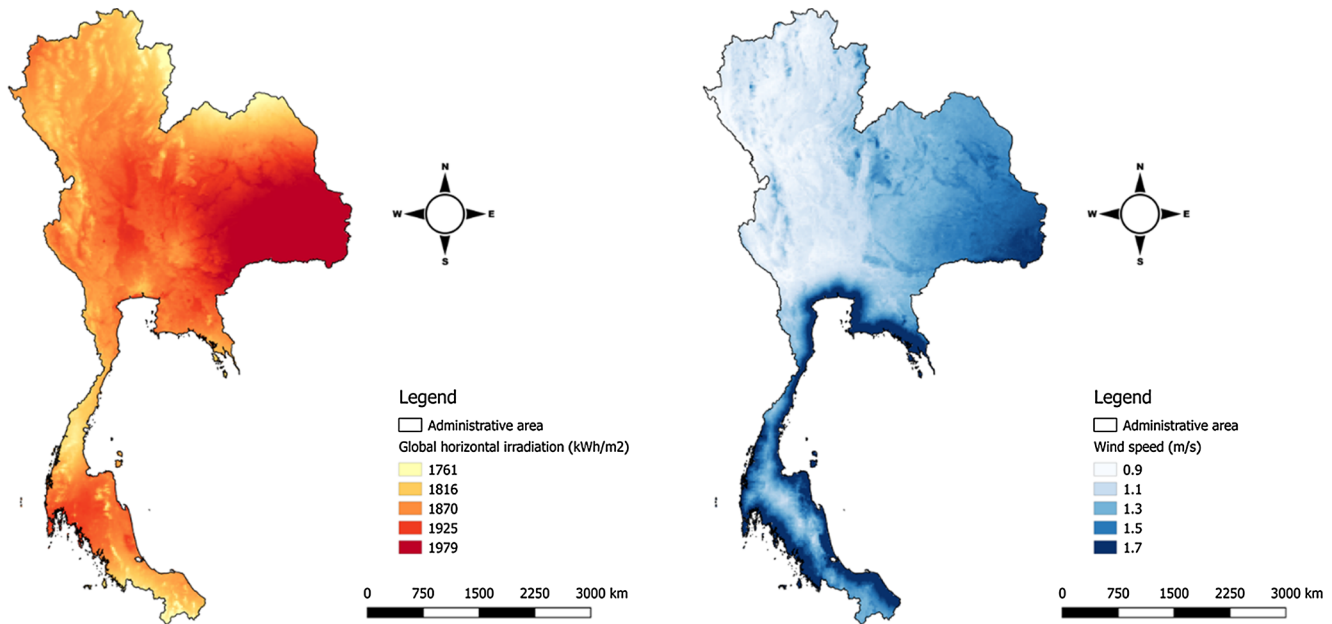

Fig. 9. Spatial distribution of the average annual global horizontal solar irradiation and wind speed in Thailand (Fick and Hijmans, 2017).

were reported in a previous study for the World Bank focused on the Southeast Asia (TrueWind Solutions, 2001) and, more recently, in the critical work carried out by Chingulpitak and Wongwises on the wind power sector in Thailand (Chingulpitak and Wongwises, 2014).

5.2.2. Off-grid and on-grid ground mounted PV system

The Pareto fronts for the PV + BATT + DG off-grid system, where the back-up power is provided by the DG, and for the on-grid system, where the back-up power is provided by the grid, are shown in Fig. 10. The *LCOE* at parity of *REL* and *RP* is significantly lower for the on-grid system, especially for *REL* and *RP* lower than 90–95%. The Pareto front point marked out by the lowest *REL* for the off-grid system corresponds the *LCOE* of the electricity produced through the diesel generator. Similarly, the Pareto front point marked out by the lowest *RP* for the on-grid system corresponds to the electricity price bought from the grid. To

a diesel price of 0.85 US$/l corresponds a *LCOE* of 0.32 US$/kWh, while the *LCOE* of the electricity taken from the grid is 0.1 US$/kWh. From Fig. 10 it can also be seen that the increase of PV electricity penetration leads to a decrease of the *LCOE* to *RP* of about 45%. That means that the *LCOE* of the electricity produced through the PV system is lower than the electricity price bought from the grid. By comparing Fig. 8 (left) and 10 (right), it is possible to compare the optimization and selection process. To avoid overproduction in off-grid system, as soon as the PV peak capacity exceeds the maximum power consumption the battery capacity starts to increase to avoid dumping the power surplus (Fig. 8(left)). On the other hand, in on-grid systems, the surplus of power production can be injected into the grid producing revenues. In this case, the battery capacity starts to increase only when the PV capacity reaches its upper bound of 200 kW$_P$ (Fig. 10(right)).
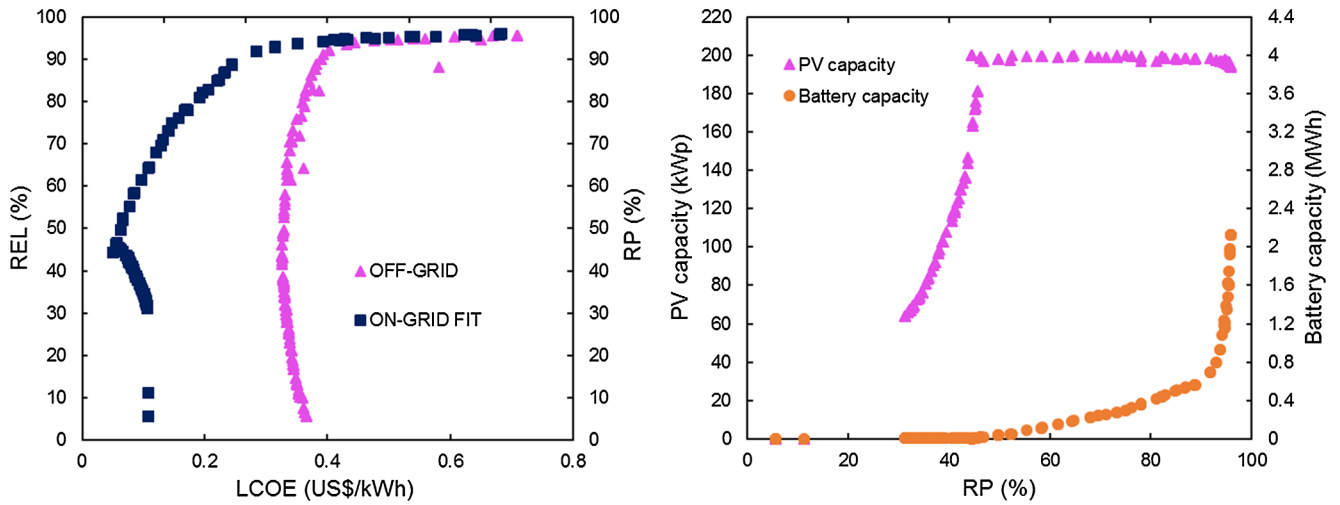
Fig. 10. Pareto fronts for the off-grid and on-grid hybrid energy system (left) and relationship between PV and battery capacities with the renewable penetration for the on-grid energy system (right).

5.2.3. Hybrid energy system: Ground mounted PV system and floating PV system (S2 and S3)

The Pareto fronts of the ground mounted PV system and floating PV system are depicted in Fig. 11. A sensitivity analysis considering
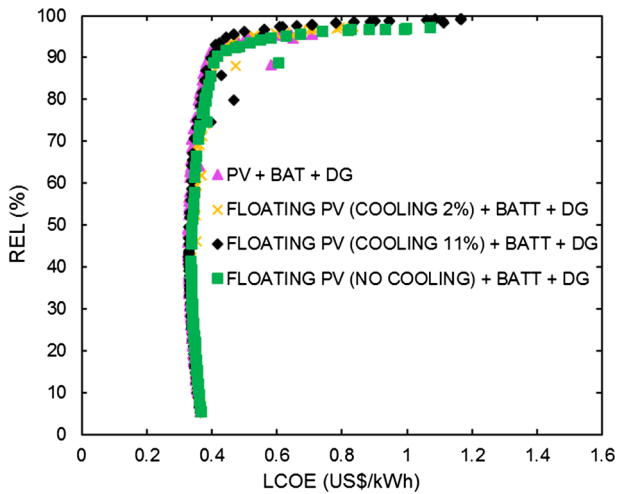

Fig. 11. Pareto front for the ground mounted and floating PV hybrid energy system.

different potential cooling effects is also taken into account. In particular, 2% and 11% increased efficiencies due to cooling effects (from Table 1) are considered. The Pareto fronts for all the investigated cases overlap except for the case FLOATING PV (COOLING 11%) + BATT + DG that at *REL* higher than 45% clearly shows a better competitiveness in terms of *LCOE* and *REL* compared to the other cases. Indeed, the higher efficiency of the floating PV system and thus the higher PV electricity production reduce the requirements for the battery capacity leading to significant cost reductions and thus lower *LCOE*. This can be clearly seen from Fig. 12 where the PV and battery capacities for the two cases are compared (the reference ground mounted PV + BATT + DG and the FLOATING PV (COOLING 11%) + BATT + DG). The higher electricity production of the floating PV system due to the cooling effect contributes to lower the PV capacity of the floating PV system compared to the ground PV system at parity of *REL*. The graph concerning the relationship between optimal battery capacity and *REL* shows that the energy storage is selected to achieve *REL* higher than 40%. It is interesting to note that to achieve *REL* higher than 90%, the storage capacity has to increase significantly from 0.7 MWh up to 2–4 MWh.

As discussed in the methodology, Section 4.3, the variation of the land cost in the study area is marked out by a wide range depending on several factors. Thus, a comprehensive sensitivity analysis has been carried out assuming different land costs, land ownerships schemes and
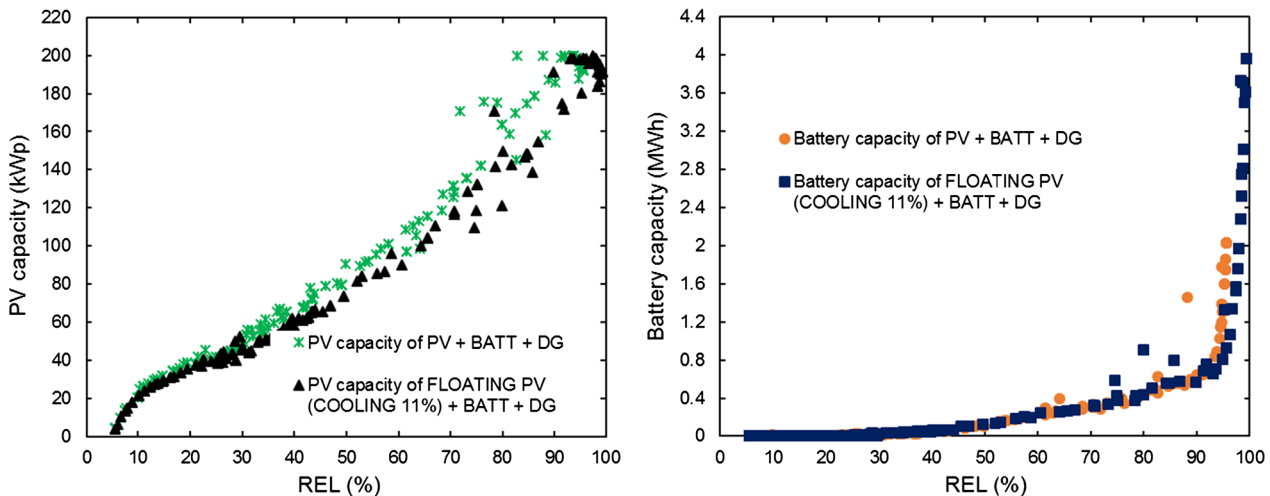

Fig. 12. Relationship between PV (left) and battery (right) capacities with the reliability for ground mounted PV system and floating PV system with 11% of increased efficiency due to cooling.
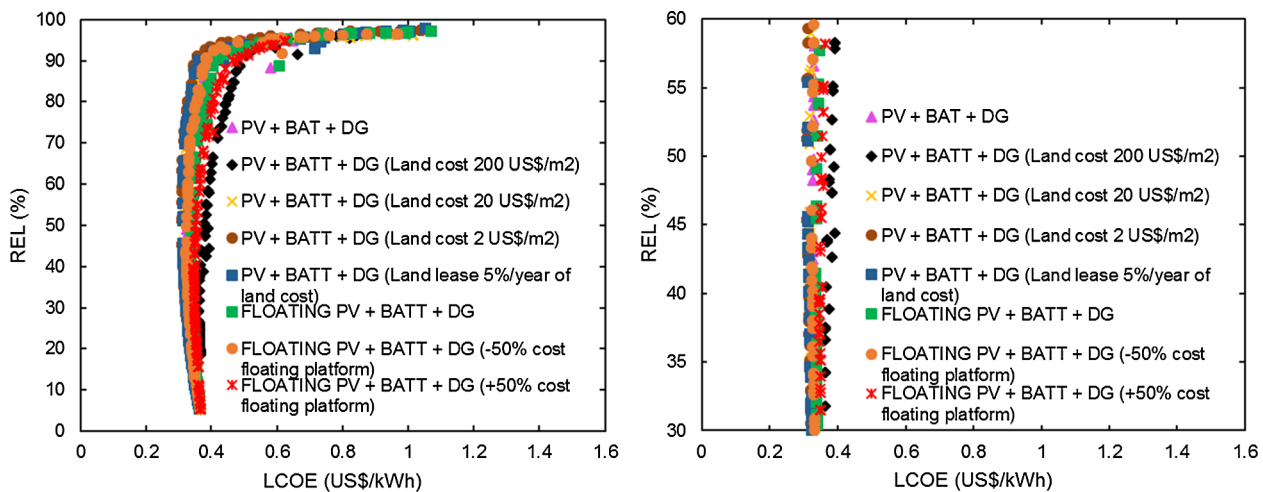
Fig. 13. Pareto fronts generated form the sensitivity analysis of land prices, land ownership, and floating PV platform (left) and detailed look for the reliabilities comprised between 30% and 70% (right).

floating PV platform costs. The summary of the sensitivity analysis is presented in Fig. 13(left). The Pareto fronts market out by the lowest and highest *LCOE* at parity of *REL* are those related to ground mounted PV systems with land leased or land at 2 US$/m² and with land bought at 200 US$/m² respectively. The third most profitable solution to support the shrimp farm operation is the floating PV system with a floating platform marked out by a specific cost 50% less than the reference case. A more detailed view of the Pareto fronts between 30% and 60% *REL* is given in Fig. 13(right).

5.2.4. Hybrid energy system: Floating PV system and floating-tracking PV (S3 and S4)

The Pareto fronts for the floating PV and floating-tracking PV systems integrated into an off-grid hybrid energy system are depicted in Fig. 14. The results do not consider any cooling effect. The floating tracking (1 axis tracking) PV hybrid system allows producing an higher amount of electricity compared to the reference floating PV system, about 5% more on annual basis. Although the higher costs of the floating-tracking PV system compared to the reference floating PV system, both solutions show similar Pareto front for *REL* up to 45%. Similar to Fig. 11, at very high *REL* the Pareto front of the floating tracking PV system shows higher competitiveness compared to the reference floating PV system due to the high specific cost of the energy storage system. At high *REL*, the increased electricity production of the

PV system becomes more important than the specific investments costs of the PV system since it allows reducing the energy storage capacity. As highlighted by Durković and Đurišić, 2017, there is limited amount of data and information concerning the economic aspects of floating-tracking PV systems due to the few commercial installations worldwide. The cost estimation and related optimization results provided in this study should thus serve as starting point for more comprehensive evaluations of floating-tracking PV systems supported by data from commercial plants.

6. Conclusions

This works has evaluated different scenarios for the decarbonization of a representative shrimp farm in Thailand. Technical, environmental and economic aspects have been considered in this study. The water-energy nexus aspects related to the implementation of floating PV systems in shrimp farms have also been discussed. A comprehensive dynamic simulation and optimization model has been developed in Matlab® environment to analyze the relationship between levelized cost of electricity and renewables reliability and penetration for off- and on-grid energy systems respectively. The key results of this study are the following:

- From a water point of view, floating PV system represents an important technological mean to reduce evaporation from the ponds of the shrimp farm. Nevertheless, from an energy point of view, the energy losses due to evaporation are minimum compared to the potential energy conversion of the installed floating PV system. Significant energy consumption reduction can be achieved considering larger areas or from a sector perspective. From a water-food-energy nexus perspective, floating PV systems can be combined in the shrimp farm sector to reduce the carbon footprint of shrimp and at the same time produce electricity for supporting the waste-water treatment consumption;
- For the selected location, PV systems represent the best solution among the investigated ones (PV system and wind turbine) to be integrated in hybrid off- and on-grid energy systems. The optimization model shows that the weak wind resources lead to a maximum renewable reliability of 15%, achieved mostly by implementing large scale batteries. From a spatial analysis perspective, the results achieved for the selected locations have a national validity due to the low/moderate wind conditions of Thailand;
- Floating PV systems represent an interesting solution to increase the profitability of PV installations, especially in locations marked out by a high cost of land. Low land prices or land leasing scheme
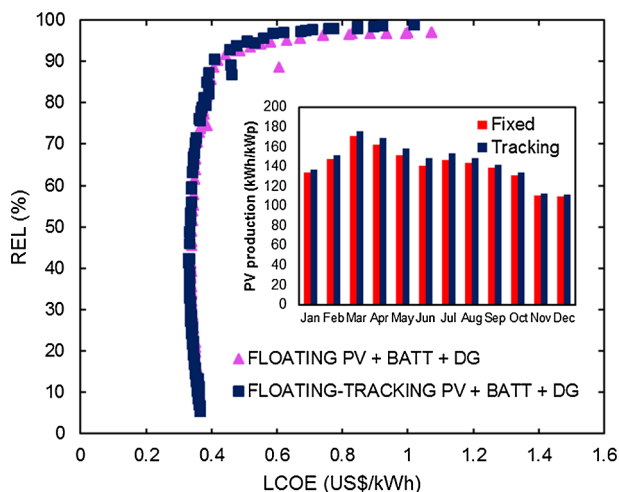

Fig. 14. Pareto front for the floating PV and floating-tracking PV hybrid energy system.

represent the most profitable solutions for PV systems making them more competitive than floating PV systems. The positive effects of cooling on the efficiency of the PV modules show that higher renewable reliabilities can be achieved at a lower levelized cost of electricity compared to ground based PV systems;

- Although floating-tracking PV systems have higher specific investment costs, the higher electricity production compared to fixed floating PV system make them competitive from a levelized cost of electricity point of view, especially for reliabilities higher than 45%.

The investigations carried out in this work led to the following recommendations. The integration of renewables in the shrimp farm sector should be mainly focused on PV systems, unless specific measurements of the wind speed show better performances for the installation of wind turbines. The possibility of having access to the grid represents the most cost-effective solution compared to off-grid systems due to the high price of diesel as back-up power. The optimal choice between different PV solutions is mainly driven by the costs of the land and floating platform. Thus, accurate estimation of those lasts two item

costs should be carried out before the investment. From a techno-economic point of view, floating and floating-tracking PV systems can be competitive to ground based PV systems even at low land prices but a detailed analysis of the cooling effects should be carried out. From an economic viewpoint, the best solution is to design hybrid energy system for renewables reliability/penetration of about 40% that guarantees the lowest levelized cost of electricity both for off- and on-grid shrimp farms.

Acknowledgements

Appendix A. Cost estimation for the floating-tracking PV system

The cost of the floating-tracking PV installation has been calculated assuming a tracking platform without a confining structure as described in Cazzaniga et al. (2018) and presented in Fig. 2. This floating-tracking PV configuration has been already implemented and tested in Italy as reported in Cazzaniga et al. (2018) and represents an ideal solution for the selected shrimp farm due to its cost-effectiveness and the confined environment. The floating structure can be realized through high-density polyethylene floating cubes with enhanced interlocking systems. The structure can be afterwards reinforced by the supporting structure of the PV modules. The main components of the installation are the following: the floating platform, the concrete anchor, the solar tracker controller, and the propulsion system. The cost for the floating PV platform, concrete anchor and the mooring system have been assumed equal to 85 US$/m^2 as for traditional floating PV systems (Santafé et al., 2014). The main difference with traditional floating PV systems is that the anchor system is installed at the bottom of the pond rather than on the edge. The cost for the solar tracker controller that actuate at least four propulsion systems has been taken from an e-commerce retailer and equal to 2,000 US$ (Alibaba, 2018). The propulsion system costs have been estimated from the propulsion system power P_p (W) given by the following equation (Molland et al., 2017):

$$P_p = \frac{P_{eff}}{\eta_p} = \frac{R_T V}{\eta_p} \tag{A.1}$$

where P_{eff} is the effective power (W), η_p is the efficiency of the propulsion system (%) (it takes into account the efficiency of the motor, gearbox, shaft and propeller), R_T is the total resistance (N), and V is the speed (m/s). The total resistance typically depends on several contributions. By assuming that the tracking system works at low speeds, the main contributions to the total resistance is given by the viscous resistance R_V and wind speed resistance R_v. The viscous resistance R_V can be calculated with the following equation (Molland et al., 2017; Remmlinger, 2014):

$$R_V = \frac{1}{2} C_V \rho_w S V^2 \tag{A.2}$$

where C_v is the coefficient of viscous resistance, ρ_w is the water density (kg/m^3), S is the wetted surface area (m^2), and V is the speed (m/s). The tracking system speed has been assumed equal to 1.0 m/s for the propulsion system capacity design. The coefficient of viscous resistance is given by the following traditional equation of hydrodynamics (Remmlinger, 2014):
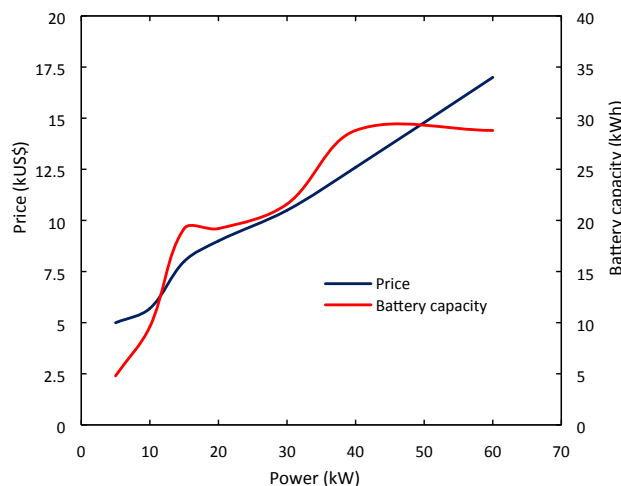

Fig. A1. Maritime propulsion system costs (OceanPlanet Energy, 2018).

Table A1

Summary of the design parameters and cost for the propulsion system of the floating-tracking PV system.

Parameter	Value	Refs./Comment
Power peak capacity (kW$_p$)	200	
Speed V (m/s)	1.0	Conservative design parameter
Drag coefficient C$_d$	1.28	Drag coefficient of a flat plate perpendicular to flow Shape effects on drag (2018)
Wind speed v (m/s)	7	See Fig. 7
Propulsion efficiency η$_P$ (%)	65	(Symington et al., 2014; Oladokun, 2015)
Propulsion system power P$_p$ (kW)	4.84 kW	Calculated with Eq. (13)
Cost of the propulsion system (kUS$)	10	Assuming to install two propulsion systems for a total capacity of 10 kW for balancing the rotational movement of the floating platform. Costs estimated from Fig. A.1

$$C_V = \frac{0.075}{[(\log_{10}R_n) - 2]^2} \tag{A.3}$$

where R_n is the Reynolds number. The wind resistance R_v is given by the drag equation:

$$R_v = \frac{1}{2}C_d\rho A v^2 \tag{A.4}$$

where C_d is the drag coefficient, ρ_a is the air density (kg/m^3), A is the area hit by the wind (m^2), and v is the wind speed (m/s). The drag coefficient has been assumed equal to 1.28 that corresponds to the drag coefficient of a flat plate perpendicular to flow (Shape effects on drag, 2018). This represents the most conservative scenario assuming that the tilt of the PV modules is equal to 90°. The interference area with the wind has been assumed equal to the area of the PV modules row along the circle radius. A wind speed of 7 m/s has been assumed as design wind speed based on the strongest wind measured at the selected location (see Fig. 7). The cost of the propulsion systems for a 200 kW$_p$ floating-tracking PV system has been estimated form the cost of an electric maritime propulsion system with energy storage depicted in Fig. A.1 (OceanPlanet Energy, 2018). A summary of the design parameters and costs for the propulsion system of the floating-tracking PV system is given in Table A.1. The corresponding specific cost of the tracking system is 60 US$/kW$_p$.

References

Chimres, N., Wongwises, S., 2016. Critical review of the current status of solar energy in Thailand. Renew. Sustain. Energy Rev. 58, 198–207. https://doi.org/10.1016/j.rser.2015.11.005.

Kumar, S., 2016. Assessment of renewables for energy security and carbon mitigation in Southeast Asia: the case of Indonesia and Thailand. Appl. Energy 163, 63–70. https://doi.org/10.1016/j.apenergy.2015.11.019.

Huenteler, J., Niebuhr, C., Schmidt, T.S., 2016. The effect of local and global learning on the cost of renewable energy in developing countries. J. Clean Prod. 128, 6–21.

Department of Alternative Energy Development and Efficiency. Energy in Thailand, Facts and Figures; 2014.

Department of Alternative Energy Development and Efficiency. Energy in Thailand: facts and figures; 2017.

Energy Policy and Planning Office. Energy Statistics; 2016.

EGAT. Electrical Generating Authority of Thailand (EGAT) https://www.egat.co.th/en/index.php?option=com_content&view=featured&Itemid=101; 2013.

FAO Yearbook. Fishery and Aquaculture Statistics-2015; 2017.

FAO Fisheries and Aquaculture Department. Available at: http://www.fao.org/fishery/topic/16140/en.

Nookuea, W., Campana, P.E., Yan, J., 2016. Evaluation of solar PV and wind alternatives for self renewable energy supply: case study of shrimp cultivation. Energy Procedia 88, 462–469. https://doi.org/10.1016/j.egypro.2016.06.026.

Sahu, A., Yadav, N., Sudhakar, K., 2016. Floating PV power plant: a review. Renew. Sustain. Energy Rev. 66, 815–824. https://doi.org/10.1016/j.rser.2016.08.051.

NREL. Floating Solar PVs Gaining Ground. Available at: https://www.nrel.gov/technical-assistance/blog/posts/floating-solar-PVs-gaining-ground.html. Accessed: 27th January 2018.

Solar Asset Management—North America. Floating solar plants: niche rising to the surface? Available at: https://solarassetmanagement.us/news-source/floating-plants-article. Accessed: 27th January 2018.

Solarplaza. Available at: https://www.solarplaza.com/channels/top-10s/11761/top-70-floating-solar-pv-plants/. Accessed: 5th November 2018.

Choi, Y.K., 2014. A study on power generation analysis of floating PV system considering environmental impact. Int. J. Softw. Eng. Appl. 8 (1), 75–84.

Majid, Z., Ruslan, M.H., Sopian, K., Othman, M.Y., Azmi, M., 2014. Study on performance of 80 watt floating photovoltaic panel. J. Mech. Eng. Sci. 7 (1), 1150–1156.

Bahaidarah, H., Subhan, A., Gandhidasan, P., Rehman, S., 2013. Performance evaluation of a PV (photovoltaic) module by back surface water cooling for hot climatic conditions. Energy 59, 445–453.

Liu, L., Wang, Q., Lin, H., Li, H., Sun, Q., Wennersten, Ronald, 2017. Power generation efficiency and prospects of floating photovoltaic systems. Energy Procedia 105, 1136–1142.

N. Yadav M. Gupta Sudhakar. Energy Assessment of Floating Photovoltaic System. In: International Conference on Electrical Power and Energy Systems (ICEPES) Maulana Azad National Institute of Technology, Bhopal, India. Dec 14-16; 2016.

Azmi, M.S.M., Othman, M.Y.H., Ruslan, M.H.H., Sopian, K., Majid, Z.A.A., 2013. Study on

electrical power output of floating photovoltaic and conventional photovoltaic. AIP Conf. Proc. 1571, 95. https://doi.org/10.1063/1.4858636.

Rosa-Clot, M., Tina, G.M., Nizetic, S., 2017. Floating photovoltaic plants and wastewater basins: an Australian project. Energy Procedia 134, 664–674.

Helfer, F., Lemckert, C., Zhang, H., 2012. Impacts of climate change on temperature and evaporation from a large reservoir in Australia. J. Hydrol. 475, 365–378.

Bengoechea, J.M., Pérez Cobos, J., Pérez Parra, J., López Segura, J.G., 1991. Evaluación de las pérdidas de agua de riego en el Campo de Dalías. Symposium sobre el agua en Andalucía. Córdoba, España.

Santafé, M.R., Soler, J.B.T., Romero, F.J.S., Gisbert, P.S.F., Gozálvez, J.J.F., Gisbert, C.M.F., 2014. Theoretical and experimental analysis of a floating photovoltaic cover for water irrigation reservoirs. Energy 67, 246–255.

Pringle, A.M., Handler, R., Pearce, J., 2017. Aquavoltaics: synergies for dual use of water area for solar photovoltaic electricity generation and aquaculture. Renew. Sustain. Energy Rev. 80, 572–584. https://doi.org/10.1016/j.rser.2017.05.191.

Engle, C.R., Mcnevin, A., Racine, P., Boyd, C.E., Paungkaew, D., Viriyatum, R., Minh, H.N., 2017. Economics of sustainable intensification of aquaculture: evidence from shrimp farms in Vietnam and Thailand. J. World Aquacult. Soc. 48 (2), 227–239. https://doi.org/10.1111/jwas.12423.

Choi, Y.K., Lee, N.H., Lee, A.K., Kim, K.J., 2014a. A study on major design elements of tracking-type floating photovoltaic systems. Int. J. Smart Grid Clean Energy 3 (1), 70–74.

Scienza Industria Tecnologia. Available at: http://www.scintec.it/ricerca/energia/ftcE.html. Accessed 19th August 2017.

Cazzaniga, R., Cicu, M., Rosa-Clot, M., Rosa-Clot, P., Tina, G.M., Ventura, C., 2018. Floating PV plants: performance analysis and design solutions. Renew. Sustain. Energy Rev. 81, 1730–1741.

Kim, S., Yoon, S., Choi, W., 2017. Design and construction of 1 MW class floating PV generation structural system using FRP members. Energies 10 (8), 1142. https://doi.org/10.3390/en10081142.

Lee, Y., Joo, H., Yoon, S., 2014. Design and installation of floating type photovoltaic energy generation system using FRP members. Sol. Energy 108, 13–27. https://doi.org/10.1016/j.solener.2014.06.033.

Y. Choi I. Kim S. Hong H. Lee. A Study on Development of Azimuth Angle Tracking Algorithm for Tracking-type Floating Photovoltaic System. doi:10.14257/astl.2014.51.45; 2014.

Choi, Y., Lee, N., Lee, A., Kim, K., 2014c. A study on major design elements of tracking-type floating photovoltaic systems. Int. J. Smart Grid Clean Energy 3 (1), 70–74. https://doi.org/10.12720/sgce.3.1.70-74.

Silvério, N.M., Barros, R.M., Filho, G.L., Redón-Santafé, M., Santos, I.F., Valério, V.E., 2018. Use of floating PV plants for coordinated operation with hydropower plants: case study of the hydroelectric plants of the São Francisco River basin. Energy Convers. Manage. 171, 339–349. https://doi.org/10.1016/j.enconman.2018.05.095.

Trapani, K., Millar, D.L., 2013. Proposing offshore photovoltaic (PV) technology to the energy mix of the Maltese islands. Energy Convers. Manage. 67, 18–26. https://doi.org/10.1016/j.enconman.2012.10.022.

Cazzaniga, R., Cicu, M., Rosa-Clot, M., Rosa-Clot, P., Tina, G.M., Ventura, C., 2017. Compressed air energy storage integrated with floating PV plant. J. Storage Mater.

13, 48–57.

Luna-Rubio, R., Trejo-Perea, M., Vargas-Vázquez, D., Ríos-Moreno, G., 2012. Optimal sizing of renewable hybrids energy systems: a review of methodologies. Sol. Energy 86 (4), 1077–1088. https://doi.org/10.1016/j.solener.2011.10.016.

Shi, Z., Wang, R., Zhang, T., 2015. Multi-objective optimal design of hybrid renewable energy systems using preference-inspired coevolutionary approach. Sol. Energy 118, 96–106. https://doi.org/10.1016/j.solener.2015.03.052.

Kaabeche, A., Diaf, S., Ibtiouen, R., 2017. Firefly-inspired algorithm for optimal sizing of renewable hybrid system considering reliability criteria. Sol. Energy 155, 727–738. https://doi.org/10.1016/j.solener.2017.06.070.

Tazvinga, H., Zhu, B., Xia, X., 2014. Energy dispatch strategy for a photovoltaic–wind–diesel–battery hybrid power system. Sol. Energy 108, 412–420. https://doi.org/10.1016/j.solener.2014.07.02.

W. Sun Life cycle assessment of indoor recirculating shrimp aquaculture system. 2009. Available at: https://deepblue.lib.umich.edu/handle/2027.42/63582. Accessed 19th August 2017.

Allen, R.G., Pereira, L.S., Raes, D., Smith, M., 1998. Crop evapotranspiration. Guidelines for computing crop water requirements, FAO.

Meteonorm. Available at: www.meteonorm.com. Accessed 19th August 2017.

Duffie, J.A., Beckman, W.A., 2013. Solar Engineering of Thermal Processes. John Wiley & Sons Ltd, Chichester.

Yingli Solar. Available at: www.yinglisolar.com/us/. Accessed: 7th June 2018.

Lydia, M., Kumar, S.S., Selvakumar, A.I., Kumar, G.E.P., 2014. A comprehensive review on wind turbine power curve modeling techniques. Renew. Sustain. Energy Rev. 30, 452–460.

Carrillo, C., Montaño, A.O., Cidrás, J., Díaz-Dorado, E., 2013. Review of power curve modelling for wind turbines. Renew. Sustain. Energy Rev. 21, 572–581.

Ismail, M.S., Moghavvemi, M., Mahlia, T.M.I., 2013. Techno-economic analysis of an optimized photovoltaic and diesel generator hybrid power system for remote houses in a tropical climate. Energy Convers. Manage. 69, 163–173.

Kanase-Patil, A.B., Saini, R.P., Sharma, M.P., 2011. Sizing of integrated renewable energy system based on load profiles and reliability index for the state of Uttarakhand in India. Renew. Energy 36 (11), 2809–2821.

OptiCE. Available at: www.optice.net. Accessed: 19th August 2018.

Martín-Chivelet, N., 2016. Photovoltaic potential and land-use estimation methodology. Energy 94, 233e242.

IRENA. Renewable power generation costs in 2014. 2015. Available at: http://www.irena.org/documentdownloads/publications/irena_re_power_costs_2014_report.pdf. Accessed: 3rd March 2017.

Lazard, Lazard's Levelized Cost of Storage Analysis, November 2017. Available at: https://www.lazard.com/media/450338/lazard-levelized-cost-of-storage-version-30.pdf.

Merei, G., Berger, C., Sauer, D.U., 2013. Optimization of an off-grid hybrid PV–wind–diesel system with different battery technologies using genetic algorithm. Sol. Energy 97, 460–473.

Global Petrol Prices. Available at: http://www.globalpetrolprices.com/Thailand/diesel_prices/. Accessed: 3rd March 2018.

IEA. Thailand Electricity Security Assessment 2016. 2017. Available at: https://www.iea.org/publications/freepublications/publication/Partner_Country_Series_Thailand_Electricity_Security_2016_.pdf. Accessed: 7th Nov 2017.

Khiareddine, A., Salah, C.B., Rekioua, D., Mimouni, M.F., 2018. Sizing methodology for hybrid PV /wind/hydrogen/battery integrated to energy management strategy for pumping system. Energy 153, 743e762.

Kaabeche, A., Ibtiouen, R., 2014. Techno-economic optimization of hybrid photovoltaic/wind/diesel/ battery generation in a stand-alone power system. Sol. Energy 103, 171–182.

HOMER. Available at:https://www.homerenergy.com/products/pro/docs/3.11/generator_lifetime.html. Accessed: 20th June 2018.

Trading Economics. Available at: http://sv.tradingeconomics.com/thailand/corporate-tax-rate. Accessed: 7th Nov 2017.

Department of Alternative Energy Development and Efficiency (DEDE), Ministry of Energy. 2015 National Survey Report of PV Power Applications in Thailand. Available at: www.iea.org.

OK Nation Blog. Available at: http://oknation.nationtv.tv/blog/meeboo/2012/09/30/entry-2. Accessed: 7th Nov 2017.

Treasury Department. Available at: http://www.treasury.go.th/main.php?filename=price_thing#. Accessed: 7th June 2018.

Portley, N., 2016. Report on the shrimp sector: Asian shrimp trade and sustainability. Sustain. Fish. Partner.

TrueWind Solutions, LCC. Wind energy resource atlas of Southeast Asia; 2001.

Chingulpitak, S., Wongwises, S., 2014. Critical review of the current status of wind energy in Thailand. Renew. Sustain. Energy Rev. 31, 312–318.

Fick, S.E., Hijmans, R.J., 2017. Worldclim 2: new 1-km spatial resolution climate surfaces for global land areas. Int. J. Climatol.

Durković, V., Ðurišić, Ž., 2017. Analysis of the potential for use of floating PV power plant on the skadar lake for electricity supply of aluminium plant in montenegro. Energies 10 (10), 1505. https://doi.org/10.3390/en10101505.

Alibaba. Available at: www.alibaba.com. Accessed: 7th June 2018.

Molland, A.F., Turnock, S.R., Hudson, D.A., 2017. Ship resistance and propulsion. Cambridge University Press.

Remmlinger, U., 2014. How to Determine the Viscous Resistance of the Delft Systematic Yacht. Hull Series.

Shape effects on drag. Available at: www.grc.nasa.gov/WWW/k-12/airplane/shaped.html. Accessed: 7th June 2018.

OceanPlanet Energy. www.bruceschwab.com/. Accessed: 7th June 2018.

Symington, W.P., Belle, A., Nguyen, H.D., Binns, J.R., 2014. Emerging technologies in marine electric propulsion. Proc. Inst. Mech. Eng., Part M: J. Eng. Maritime Environ. 230 (1), 187–198. https://doi.org/10.1177/1475090214558470.

Oladokun, S.O., 2015. Study of efficiency and environmental performance of propeller. J Coast Zone Manag 18, 400. https://doi.org/10.4172/2473-3350.1000400.